

# Statistical Self-Similarity of One-Dimensional Growth Processes

Michael Prähofer and Herbert Spohn

Zentrum Mathematik and Physik Department, TU München, D-80290 München, Germany. Email: *praehofer@ma.tum.de*, *spohn@ma.tum.de*

**Abstract.** For one-dimensional growth processes we consider the distribution of the height above a given point of the substrate and study its scale invariance in the limit of large times. We argue that for self-similar growth from a single seed the universal distribution is the Tracy-Widom distribution from the theory of random matrices and that for growth from a flat substrate it is some other, only numerically determined distribution. In particular, for the polynuclear growth model in the droplet geometry the height maps onto the longest increasing subsequence of a random permutation, from which the height distribution is identified as the Tracy-Widom distribution.

PACS numbers: 02.50.Ey, 68.35.Ct

## 1. Introduction

Quite analogous to equilibrium systems close to their critical point, growth processes exhibit statistical self-similarity and scaling. Their theoretical investigation is a continuing enterprise for a variety of reasons. Perhaps the most fundamental one is that statistical self-similarity emerges from the dynamical rules without any particular fine-tuning, which is believed to be a basic characteristic of many nonequilibrium systems [1, 2, 3]. The persisting theoretical challenge is to develop renormalization group type methods which have been so powerful in the understanding of equilibrium critical phenomena.

In the context of KPZ theory [4] most of the recent efforts have concentrated on scaling exponents and in particular on the question of an upper critical dimension [5, 6, 7, 8]. In this note we will focus on the full height distribution at one point above the substrate. In addition we will restrict ourselves to one-dimensional growth processes, where *static* fluctuations are the same as in equilibrium due to a fluctuation-dissipation property, i.e. the roughness exponent is known to be  $\frac{1}{2}$ .

The most commonly adopted set-up is to start from a flat substrate, i.e., if  $h(x, t)$  denotes the height above  $x \in \mathbb{R}$  at time  $t$ , then initially  $h(x, 0) = ux$  with slope  $u$ .  $h(x, t)$ ,  $t > 0$ , is random through the dynamical rules which will have to be specified for a concrete model. The slope  $u$  is a locally conserved quantity. By translation invariance,  $h(x, t) - ux$  has a distribution independent of  $x$  and we may consider the

height  $H(t) = h(0, t)$  above the origin. For large times it will increase linearly with time with a slope dependent growth velocity  $v(u)$ .  $H(t)$  fluctuates on the scale  $t^{1/3}$ . Therefore

$$H(t) = v(u)t + C(u)t^{1/3}\xi \quad (1)$$

for large  $t$ . The random variable  $\xi$  is of order one and independent of  $t$  and  $u$ . Equation (1) should be viewed in analogy to the central limit theorem for a random walk with independent increments. In that case  $v(u)$  would be the average drift, the fluctuations diffusive on the scale  $t^{1/2}$ , and  $\xi$  a standard Gaussian random variable.

Following Krug *et al* [9], the prefactor  $C(u)$  depends only on macroscopic properties of the growth model, namely the leading nonlinear part of the slope dependent growth velocity,  $\lambda(u) = v''(u)$ , and the static susceptibility or roughness amplitude,

$$A(u) = \lim_{x \rightarrow \infty} \lim_{t \rightarrow \infty} x^{-1} \langle (h(x, t) - h(0, t) - ux)^2 \rangle, \quad (2)$$

with limits in this order. On dimensional grounds we must have then

$$C(u) = \text{sign}(\lambda(u)) (a|\lambda(u)|A(u)^2)^{1/3}, \quad (3)$$

where  $a$  is a dimensionless number, independent of  $u$ , fixing the absolute scale of  $\xi$ . Krug *et al* [9] have studied  $\xi$  on the level of moments for a variety of growth models, thereby strongly supporting the claim that the scaling form (1) together with (3) is the same for all growth models in the KPZ universality class.

In the very early studies on growth models, like the Eden model, one started with a single seed at the origin to have a cluster growing through irreversible aggregation. For large times the droplet grows then self-similarly with a shape depending on the particular dynamical rule. In fact the macroscopic shape is determined through the slope dependent growth velocity by the Wulff construction, i.e. growth velocity and shape are related as surface tension and crystal shape in equilibrium. Thus, as for a flat substrate, in the droplet geometry there is self-similar growth, but now with a (macroscopically) non-vanishing curvature. The analogue of (1) is the distance of the surface from the origin along a given ray and it is natural to expect for it the scaling form

$$R(t) = vt + Ct^{1/3}\chi \quad (4)$$

with some universal random variable  $\chi$ .

The main part of our note studies the shape fluctuations (4) in the droplet geometry. In Section 2 we show that for the polynuclear growth (PNG) model (see for example [11] and references therein)  $\chi$  has the Tracy-Widom (TW) distribution appearing in the theory of random matrices. We give some numerical and analytical support for the universality hypothesis. In addition, we clearly demonstrate that  $\xi \neq \chi$ . Thus for self-similar growth with zero noise initial conditions there are two distinct classes, flat substrate (zero curvature) and droplet (non-zero curvature). In both geometries the height has the scaling form (1), resp. (4), but the universal random variables  $\xi$  and  $\chi$  have different distributions.

## 2. The PNG droplet

The PNG model describes a crystal growing layer by layer on a one-dimensional substrate through random deposition of particles. They nucleate on existing plateaus of the crystal forming new islands. In an idealization these islands spread laterally with constant speed by steady condensation of further material at the edges of the islands. Adjacent islands of the same level coalesce upon meeting and on top of the new levels further islands emerge.

Nucleation events occur independently and uniformly in space-time. Given the space-time coordinates  $(x_0, t_0)$ ,  $x_0 \in \mathbb{R}$ ,  $t_0 > 0$ , of such an event, the corresponding island nucleates in level

$$h_0 = h(x_0, t_0) + 1 \tag{5}$$

in units of transverse lattice spacings. We also choose the time unit such that the lateral growth speed equals one. To determine the height  $h(x, t)$  we note that it depends only on the nucleation events in the backward light cone of  $(x, t)$ . We label them as  $(x_n, t_n)$ ,  $n = 1, 2, \dots$ . Then

$$h_n = h(x_n, t_n) + 1, \quad n = 1, 2, \dots, \tag{6}$$

according to (5), and  $h(x, t)$  is obtained as the maximum over all  $h_n$  in the backward light cone,

$$h(x, t) = \max\{h_n : n = 1, 2, \dots, |x - x_n| < t - t_n\}, \tag{7}$$

with the rule that  $h(x, t) = 0$  if there is no such nucleation event. (6) and (7) together define recursively all  $h_n$  and therefore  $h(x, t)$ .

For droplet growth on the initially flat substrate, a single island starts spreading from the origin and further nucleations take place only above this ground layer which we define to have zero height. We want to study the probability distribution of  $h(x, t)$ , i.e.  $\text{Prob}\{h(x, t) = n\}$  for  $n = 0, 1, 2, \dots$ ,  $|x| < t$ . Clearly  $h(x, t)$  is determined by the set of nucleation events inside the rectangle  $R_{(x,t)} = \{(x', t') \in \mathbb{R}^2 : |x'| \leq t' \text{ and } |x - x'| \leq t - t'\}$ . In light-like coordinates,  $u = (t' + x')/\sqrt{2}$ ,  $v = (t' - x')/\sqrt{2}$ , the rectangle  $R_{(x,t)}$  equals  $[0, U] \times [0, V]$  with  $U = (t + x)/\sqrt{2}$ ,  $V = (t - x)/\sqrt{2}$ . The nucleation events in  $R_{(x,t)}$  are Poisson distributed with density one. We label them as  $(u_n, v_n)$ ,  $n = 1, \dots, N$ ,  $N$  random, such that  $0 \leq u_1 < \dots < u_N \leq U$ . The corresponding order in the second coordinate  $v$ ,  $0 \leq v_{p(1)} < \dots < v_{p(N)} \leq V$ , defines then (with probability one) a permutation  $p$  of length  $N$ , compare with Figure 1. In order to distinguish nucleation events corresponding to different height levels, we partition  $(p(1), \dots, p(N))$  into decreasing subsequences according to the following algorithm. For the first subsequence one starts with the first entry in the tuple and, scanning from left to right, one adds an entry to the subsequence if it is smaller than the so far last entry in this subsequence. Every used entry is marked as deleted. When the end of the tuple is reached the first subsequence is completed. This procedure is repeated to obtain further subsequences by using only the undeleted entries of the

original tuple. As a result the permutation  $p$  is partitioned into decreasing subsequences. The nucleation events of each such subsequence are on the same height level and distinct subsequences correspond to distinct heights. The space-time height lines, across which  $h(x', t')$  increases by one unit, are thus constructed by connecting the nucleation events belonging to the same subsequence by a zigzag line, as depicted in Figure 1. In this

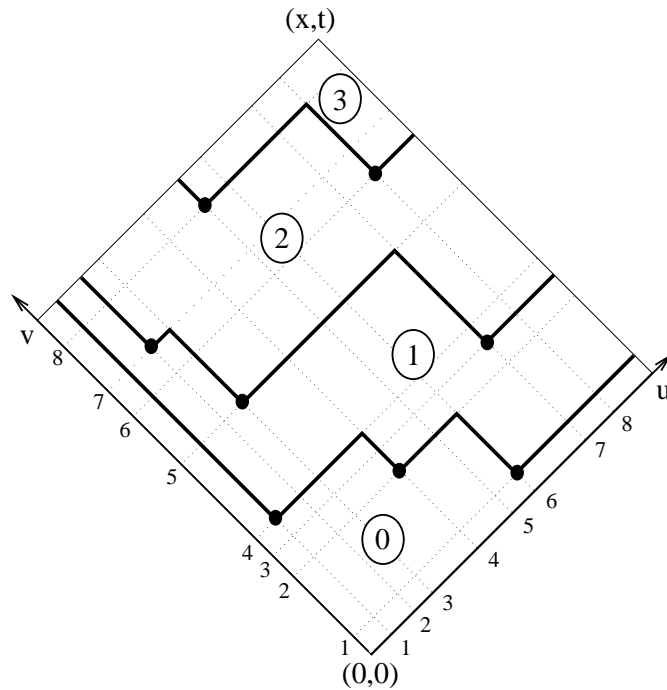


**Figure 1.** Space-time picture of a tiny PNG droplet

example we have the permutation  $(4, 7, 5, 2, 8, 1, 3, 6)$ . The decreasing subsequences are  $(4, 2, 1)$ ,  $(7, 5, 3)$ ,  $(8, 6)$ . They define three height lines. For an arbitrary permutation  $p$ ,  $h(x, t)$  equals the number of decreasing subsequences, which is precisely the length,  $l$ , of the *longest increasing subsequence* of  $p$ . To see this take any increasing subsequence of  $p$ . By construction every element of this subsequence belongs to a different height line. Therefore  $l \leq h(x, t)$ . The reverse inequality is obtained by noticing that a nucleation event  $(i, p(i))$  at level  $k + 1$  is necessarily situated in the forward light cone of at least one nucleation event  $(j, p(j))$  at level  $k$ , i.e.  $i > j$  and  $p(i) > p(j)$ .  $(j, p(j))$  is called a predecessor of  $(i, p(i))$ . Since there is at least one nucleation event in level  $h(x, t)$ , successive selections of predecessors in consecutive levels result in an increasing subsequence of length  $h(x, t)$ , therefore  $l \geq h(x, t)$ .

In fact, the mapping described here has been used before in [12], where the authors consider the Hammersley process [13] in order to study the asymptotics of  $l$  as  $N \rightarrow \infty$ . We remark that the world lines of particles in the Hammersley process are exactly the space-time step lines of the PNG model, after a rotation of  $45^\circ$  together with an appropriate adjustment of the boundary conditions. To our knowledge this simple observation has not yet been reported in the literature and establishes a connection

between the two models in much the same way as between the simple exclusion and the zero-range processes [14].

For given  $N$  the nucleation events are uniformly and independently distributed in the rectangle  $R_{(x,t)}$ . Since the  $u$ - and  $v$ -integrations factorize, this induces the uniform distribution on the set of all permutations of length  $N$ . By the Poisson law,  $N$  has the probability distribution

$$P(N) = \exp(-\lambda) \frac{\lambda^N}{N!}, \quad \lambda = UV = (t^2 - x^2)/2, \quad N = 0, 1, \dots \quad (8)$$

Thus the height of the PNG droplet is equal to the length of the longest increasing subsequence of a random permutation with Poisson distributed length, which for a fixed length of the permutation is known as Ulam's problem [15].

In recent years there has been spectacular advance on Ulam's problem, for a survey see [16]. One important element are deep combinatorial identities expressing the probability distribution of  $l$  through quantities known from the theory of random matrices. In our particular context the identity reads

$$\text{Prob}\{l(\lambda) = n\} = \frac{\exp(-\lambda)}{n!(2\pi)^n} \int_{[-\pi, \pi]^n} \exp\left(2\sqrt{\lambda} \sum_{j=1}^n \cos \theta_j\right) \prod_{1 \leq j < k \leq n} |e^{i\theta_j} - e^{i\theta_k}|^2 d^n \theta, \quad (9)$$

which corresponds to the partition function for the eigenvalues in the unitary ensemble with an external cosine potential. Baik *et al* [17] succeeded to extract from (9) the  $\lambda \rightarrow \infty$  asymptotics with the results

$$l(\lambda)/\sqrt{\lambda} \rightarrow 2 \quad \text{in probability} \quad (10)$$

and

$$\frac{l(\lambda) - 2\sqrt{\lambda}}{\lambda^{1/6}} \rightarrow \chi \quad \text{in distribution,} \quad (11)$$

together with the convergence of moments. Here  $\chi$  is a random variable, whose distribution is the famous Tracy-Widom (TW) distribution of the properly shifted and rescaled largest eigenvalue of a GUE distributed random matrix [18].  $\chi$  has the distribution function

$$F(t) = \exp\left(-\int_t^\infty (x-t)u(x)^2 dx\right), \quad (12)$$

where  $u(x)$  is the unique solution of the Painlevé II equation,

$$u'' = 2u^3 + xu, \quad (13)$$

with the asymptotic boundary conditions  $u(x) \sim \text{Ai}(x)$  as  $x \rightarrow \infty$ ,  $\text{Ai}(x)$  being the Airy function [19]. The probability density,  $F'(t)$ , of  $\xi$  has the asymptotics  $\ln F'(t) \simeq -|t|^3/12$  for  $t \rightarrow -\infty$  and  $\ln F'(t) \simeq -\frac{4}{3}t^{3/2}$  for  $t \rightarrow \infty$ .

We remark that the connection of the right-hand side of equation (9) to the Painlevé II equation has been established on an heuristic level already in the context of unitary-matrix models [20].

To come back to the PNG droplet we only have to use that  $h(x, t) = l(\lambda)$  and to translate (10) and (11) into the surface picture. Equation (10) states that the droplet acquires for large times a deterministic ellipsoidal shape given by

$$\lim_{t \rightarrow \infty} t^{-1} h(ct, t) = \sqrt{2} \sqrt{1 - c^2}. \quad (14)$$

for  $-1 \leq c \leq 1$ . Thus with our particular initial conditions the PNG model grows in the form of a droplet. The second result ensures that the shape fluctuations are on the scale  $t^{1/3}$  and in addition identifies the limiting distribution,

$$\lim_{t \rightarrow \infty} \frac{h(ct, t) - t\sqrt{2}\sqrt{1 - c^2}}{(t\sqrt{(1 - c^2)/2})^{1/3}} = \chi. \quad (15)$$

Note that in (15) only the asymptotic average is subtracted. Therefore  $\chi$  may have a mean different from zero, which is indeed the case, as can be seen in Figure 2, where the TW distribution  $F'(t)$  is plotted on a semi-logarithmic scale.

### 3. Flat substrate

For flat initial conditions, by translational invariance, it suffices to study the distribution of the height above the origin, i.e.  $H(t) = h(0, t)$ . At first glance, since the droplet curvature vanishes on the microscopic scale, one would expect the distributions for  $\xi$  in Equation (1) and for  $\chi$  in Equation (4) to be identical. To better understand this point we again consider the PNG model.

The flat initial conditions in the PNG model are  $h(x, 0) = 0$  and nucleation is now allowed everywhere on the line. We consider  $H(t) = h(0, t)$ .  $H(t)$  depends on nucleation events in the backward light cone of  $(0, t)$ , i.e. in the triangle  $T_t = \{(x', t'); 0 \leq t' < t, |x'| < t'\}$ . As before we construct a random permutation from the nucleation events inside  $T_t$  and  $H(t)$  equals the length of the longest increasing subsequence. Unfortunately the induced measure on the permutations is no longer uniform and the analogue of (9) does not seem to be known.

To relate  $H(t)$  to the distribution  $h(0, t)$  of the height process from the PNG droplet we define  $H_x(t)$ ,  $|x| \leq t$  as the height which results if the height lines are constructed from nucleation events inside the rectangle  $\{(x', t') : |x'| \leq t - t' \text{ and } |x - x'| \leq t'\}$  only. Since a longest increasing subsequence of nucleation events for  $H(t)$  must be contained in at least one of these rectangles, we have  $H(t) = \max_{|x| \leq t} H_x(t)$ . Now for a given set of nucleation events in  $T_t$  the mapping  $t' \mapsto t - t'$ ,  $x' \mapsto -x'$  yields a realization of nucleation events for the PNG droplet up to time  $t$ . The algorithm to determine  $h(x, t)$ ,  $|x| \leq t$ , for the droplet involves the same permutation as for  $H_x(t)$ , only the partition has to be into *increasing* subsequences starting from the *right*. Nevertheless  $h(x, t)$  equals the longest increasing subsequence (from the left) by the same reasoning as in Section 2. As a result we have the alternative expression

$$H(t) = \max_{|x| \leq t} h(t, x) \quad \text{in distribution,} \quad (16)$$

where  $h(x, t)$  is the height process from the PNG droplet.

We note that the maximum is taken among highly correlated random variables. To model their statistics we assume local stationarity and write for the height of the droplet  $h(x, t) = h(0, t) - x^2/(t\sqrt{2}) + b(x)$  in the vicinity of  $x = 0$ , where  $b(x)$  is a two sided random walk with  $b(0) = 0$ , zero mean and the covariance  $\langle b(x)^2 \rangle \propto |x|$ , as long as  $x = o(t)$ . Therefore the maximum in (16) is achieved inside a region of order  $t^{2/3}$  around  $x = 0$  and the modifications between the distributions of  $H(t)$  and  $h(0, t)$  are on the scale  $t^{1/3}$ . Our argument suggests that  $\chi \neq \xi$ , which is indeed supported by the numerical simulations of Section 5. In addition it points at a close but non-trivial connection between the distributions  $\xi$  and  $\chi$  which might pave the way for an analytical description of  $\xi$ .

#### 4. Universality

As explained in the Introduction, when starting with a flat substrate of slope  $u$ , the height at the origin scales as

$$H(t) = v(u)t + C(u)t^{1/3}\xi. \quad (17)$$

$v(u)$  and  $C(u)$  are non-universal parameters which depend on the slope  $u$  and have to be computed separately for each model according to the definition in (3) and above. However,  $\xi$  is universal under the stated initial conditions.

Clearly it is desirable to have a corresponding scaling form for droplet growth, the combining feature being the scale invariance of the macroscopic shape, which means that for large  $l$  we have

$$\bar{h}(lx, lt) = l\bar{h}(x, t) \quad (18)$$

with  $\bar{h}$  denoting the deterministic profile. For a flat substrate (18) holds trivially, whereas for a droplet the shape is determined by the Wulff construction (see for example [21]). In other words, the deterministic growth equation

$$\partial_t \bar{h}(x, t) = v(\partial_x \bar{h}(x, t)) \quad (19)$$

with the inclination dependent growth velocity  $v$  allows only for two types of self-affine solutions, the flat surface with slope  $u$ ,  $\bar{h}(x, t) = tv(u) + xu$  and the droplet

$$h(ct, t) = tf(c), \quad (20)$$

where  $f$  solves the equation  $f(c) - cf'(c) = v(f'(c))$ . The parameter  $c$  is related to the local slope  $u = f'(c)$  by  $c = -v'(u)$ . In view of (17) we are therefore led to the universal scaling law for the height distribution of a growing droplet

$$h(ct, t) = tf(c) + \text{sign}(\lambda)(\frac{1}{2}|\lambda|A^2t)^{1/3}\chi. \quad (21)$$

Here  $\chi$  is a random variable with TW distribution.

With the rigorous result (15) we are in the position to check the scaling form (21) for the PNG droplet. In the steady states of the PNG model the left and right island edges (steps) have an independent Poisson distribution whose strength is determined by the average slope [22, 23]. With this information one obtains, in our units, the slope

dependent growth velocity  $v(u) = \sqrt{2+u^2}$ , yielding  $\lambda = 2/(2+u^2)^{-2/3}$ , and the static roughness amplitude  $A = v(u)$ . The relation  $c = -u/\sqrt{2+u^2}$  is invertible, therefore one can write  $\lambda A^2 = \sqrt{2(1-c^2)}$ . Comparing with (15) we see that (21) is indeed satisfied for the PNG droplet. In addition, with the definition (12) of the TW distribution, the dimensionless scale factor, denoted by  $a$  in Equation (3), is fixed to be  $\frac{1}{2}$ .

In a remarkable paper [24] Johansson treats the totally asymmetric simple exclusion process (TASEP) by a similar but somewhat more involved mapping to increasing subsequences in generalized permutations. Interpreted as a one-dimensional discrete growth model it describes a crystal occupying initially three quadrants of the plane. Further particles, represented as unit squares, may nucleate only if at least two nearest neighbors are already occupied. Thus the crystal grows into the forth quadrant starting from the origin. It has been known for some time [25] that on a macroscopic scale the shape becomes deterministic. Johansson proves a scaling law similar to (15) with the same limiting distribution, but a negative prefactor. In the TASEP particles jump, subject to the exclusion constraint, to the right with rate 1. Since the stationary measures are Bernoulli, one has  $v(u) = \frac{1}{4}(1-u^2)$ ,  $|u| \leq 1$  and  $A(u) = \frac{1}{4}(1-u^2)$ . Inserting in (21), we recover the result of Johansson, the negative prefactor coming from  $\lambda(u) = -\frac{1}{2}$ . This is one of the few instances where universality has been rigorously established on the level of distributions.

## 5. Numerics

In Figure 2 we compare the two distributions of  $\chi$  and  $\xi$  in a semi-logarithmic plot. The TW distribution, which is drawn as a solid line, is obtained by numerically solving (13). Its mean is  $-1.771087$  and its variance is  $0.813195$ . For the skewness,  $\langle \chi^3 \rangle_c / \langle \chi^2 \rangle_c^{3/2}$ , and the kurtosis,  $\langle \chi^4 \rangle_c / \langle \chi^2 \rangle_c^2$ , one obtains  $0.2241$  and  $0.09345$ , respectively. Here  $\langle \chi^k \rangle_c$  denotes the  $k$ -th cumulant (fully truncated moment). Superimposed are the empirical distributions determined at various times, ranging from 1000 to 2000 units, from a Monte-Carlo simulation of the PNG droplet. Finite time effects are most pronounced for the first moment. At  $t = 2000$  there is still a noticeable deviation of about 3% which seems to fade away very slowly. The other quantities agree with the exact values within the statistical fluctuations.

Since for the distribution of  $\xi$  there is no analytic expression available, we performed Monte Carlo simulations of the continuum PNG model for flat and equidistantly stepped initial conditions. We used slopes  $0$ ,  $\frac{1}{2}$  and  $1$ , up to only moderate times  $t \leq 2500$  on an effectively infinite substrate. The number of independent runs were around 10 000 for each slope, but due to translation invariance the number of sample points is about  $10^7$  for each recorded time. From our data we estimate the mean, variance, skewness, and kurtosis of  $\xi$  as  $-0.76(1)$ ,  $0.637(3)$ ,  $0.29(1)$ , and  $0.16(1)$ , respectively. In view of the slow convergence of the first moment for the PNG droplet the estimate for  $\langle \xi \rangle$  has to be taken with care, since it might not yet have reached its true asymptotic value. Our values are consistent with earlier studies of  $\xi$  for various growth models [9, 10].

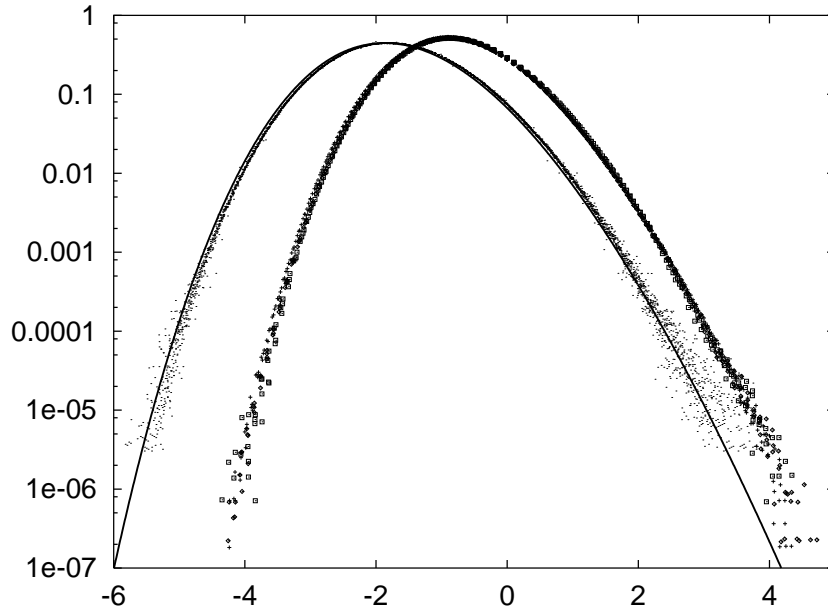


**Figure 2.** Semi-logarithmic plot of the scaled height distributions. The solid line is the Tracy-Widom distribution. Superimposed are Monte Carlo results for the PNG droplet. The right data points are Monte Carlo results for the flat case as explained in the text.

So far we started the growth process with a deterministic height profile. An obvious variant is to start with a random configuration. The most natural choice is to take a stationary height statistics obtained in the long time limit. If  $h(x, t)$  denotes this stationary growth process (i.e. the statistics of  $\partial_x h(x, t)$  depends only on space-time differences), then as before

$$h(v'(u)t, t) - h(0, 0) \simeq v(u)t + C(u)t^{1/3}\eta \quad (22)$$

for large  $t$ . Along a trajectory with slope different from  $v'(u)$  one has ordinary diffusive scaling as  $t^{1/2}$  due to the static roughness of the height profile. Our simulations (not shown) yield, the mean being zero by definition, 1.476(7), 0.375(5), and 0.31(1) for the variance, skewness, and kurtosis of  $\eta$ , which again is consistent with [9] and [10].

## 6. Conclusions

We have identified three distinct universal distributions: growth with noisy stationary initial data, and curved and flat growth from deterministic initial data. In addition we have pointed out that the height of the PNG droplet is simply related to the statistics of the length of the longest increasing subsequence of a random permutation. This leads to a complete characterization of the macroscopic shape and of the fluctuations in the height above a single reference point.

It is somewhat unexpected to have the links one-dimensional surface growth to random permutations to random matrices. As a first introduction to the latter

we recommend the survey paper by Aldous and Diaconis [16]. Longest increasing subsequences arise there in the context of solitaire or patience card games. In patience sorting a well shuffled deck of  $N$  cards, labeled  $1, 2, \dots, N$ , is dealt into piles according to the, admittedly somewhat boring, two rules: (i) A low card is always placed on the leftmost pile with a higher card on top. (ii) If (i) cannot be achieved, a new pile is started to the right of the previous piles. The connection to the PNG model is immediate. A pile of cards corresponds to a height line, the pile size is the number of nucleation events on the height line, and, of course, the number of piles is the height. As regards to surface growth it would be of great interest to further exploit the random matrix theory in the computation of universal properties and to extend this technique to higher dimensions.

### Acknowledgments

We thank Craig Tracy for providing us with the Mathematica<sup>®</sup> code for the TW distribution.

### Addendum

In the meantime we have noted that the scaling distribution  $\xi$  for a flat substrate is the limiting distribution of the largest eigenvalue of a GOE distributed random matrix [26]. More precisely, the distribution function of  $\xi$  is given by

$$F(2^{2/3}t) = \exp\left(-\frac{1}{2}\int_t^\infty (x-t)u(x)^2 dx - \frac{1}{2}\int_t^\infty u(x)dx\right). \quad (23)$$

Its first four cumulants are  $-0.76007$ ,  $0.63805$ ,  $0.2935$ , and  $0.1652$ . Our proof uses the symmetrized random permutations studied by Baik and Rains [27]. We are grateful to Percy Deift and Craig Tracy for pointing out this reference to us.

### References

- [1] A.-L. Barabási and H. E. Stanley, *Fractal Concepts in Surface Growth* (Cambridge University Press, Cambridge, 1995)
- [2] P. Bak, *How Nature Works* (Copernicus Books, 1995)
- [3] U. Frisch, *Turbulence; A Legacy of A. N. Kolmogorov* (Cambridge University Press, Cambridge, 1995)
- [4] M. Kardar, G. Parisi, and Y.-Z. Zhang, Phys. Rev. Lett. **56**, 889 (1986).
- [5] M. Lässig and H. Kinzelbach, Phys. Rev. Lett. **78**, 903 (1997)
- [6] T. J. Newman and M. R. Swift, Phys. Rev. Lett. **79**, 2261 (1997)
- [7] M. Lässig, J. Phys. C **10**, 9905 (1998).
- [8] C. Castellano, M. Marsili, M. A. Muñoz, and L. Pietronero, Phys. Rev. E **59**, 6460 (1999)
- [9] J. Krug, P. Meakin, and T. Halpin-Healy, Phys. Rev. A **45**, 638 (1992).
- [10] J. M. Kim, M. A. Moore, and A. J. Bray, Phys. Rev. A **44**, 2345 (1991).
- [11] E. Ben-Naim, A. R. Bishop, I. Daruka, and P. L. Krapivsky, J. Phys. A: Math. Gen. **31**, 5001 (1998).
- [12] D. Aldous and P. Diaconis, Prob. Th. and Rel. Fields. **103**, 199 (1995).

- [13] J. M. Hammersley, in *Proc. 6th Berkeley symp. math. statist. and probability*, Vol. 1, 345, University of California Press, 1972.
- [14] T. M. Liggett, *Interacting Particle Systems* (Springer Verlag, New York, 1985)
- [15] S. M. Ulam, in *Modern Mathematics for the Engineer*, E. F. Beckenbach, ed., McGraw-Hill, 1961.
- [16] D. Aldous and P. Diaconis, *Bull. Amer. Math. Soc.* **36**, 413 (1999)
- [17] J. Baik, P. Deift, and K. Johansson, LANL E-print math.CO/9810105.
- [18] C. A. Tracy and H. Widom, *Comm. Math. Phys.* **159**, 151 (1994).
- [19] S. P. Hastings and J. B. McLeod, *Arch. Rat. Mech. Anal.*, **73**, 31 (1980).
- [20] V. Periwal and D. Shevitz, *Phys. Rev. Lett.* **64**, 1326 (1990).
- [21] J. Krug and H. Spohn, in *Solids far from equilibrium*, ed. C. Godrèche, (Cambridge University Press, Cambridge 1992)
- [22] C. H. Bennett, M. Büttiker, R. Landauer, and H. Thomas, *J. Stat. Phys.* **24**, 419 (1981).
- [23] J. Krug and H. Spohn, *Europhys. Lett.* **8**, 219 (1989).
- [24] K. Johansson, LANL E-print math.CO/9903134.
- [25] H. Rost, *Z. Wahrsch. Verw. Gebiete* **58**, 41 (1981).
- [26] C. A. Tracy and H. Widom, *Comm. Math. Phys.* **177**, 727 (1996).
- [27] J. Baik and E. M. Rains, LANL E-print math.CO/9910019.